RSC Advances

ROYAL SOCIETY OF CHEMISTRY

www.rsc.org/advances

Table of Contents Graphic and Synopsis

The chemical structures of dispersants have a crucial effect on the dispersion of single-walled carbon nanotubes (SWCNTs). *Poly*((furfuryl methacrylate)-*co*-(2-(dimethylamino)ethyl methacrylate)) (*p*(FMA-*co*-DMAEMA) has limited applications, although it could be dispersed SWCNTs in THF. To dispersed SWCNTs in different polar solvents, *p*(FMA-*co*-DMAEMA) was quaternized *p*(FMA-*co*-DMAEMA) (*p*(FMA-*co*-*Q*DMAEMA)) using simple chemistry. The modified dispersant *p*(FMA-*co*-*Q*DMAEMA) changed solubility in solvents and the dispersibility of SWCNTs. SWCNTs dispersed well in polar solvents, such as ethylene glycol, methanol, water and DMF, using *p*(FMA-*co*-*Q*DMAEMA).

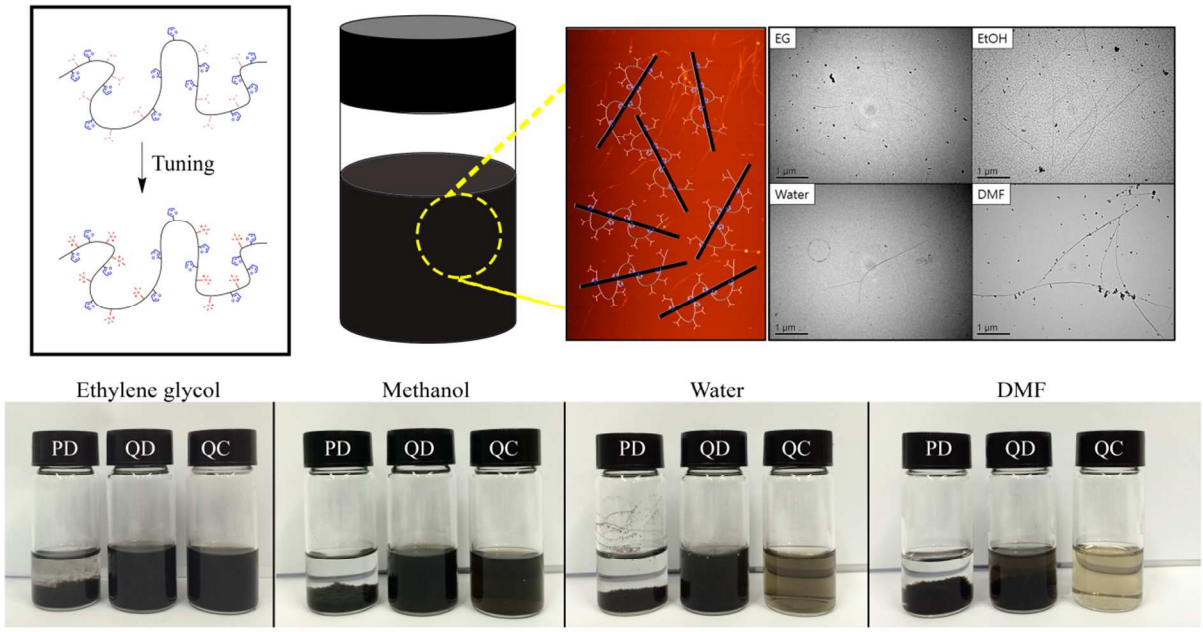

Journal Name

ARTICLE

Received 00th January 20xx,

Accepted 00th January 20xx

DOI: 10.1039/x0xx00000x

www.rsc.org/

Facile Tuning of a Polymeric Dispersant for Single-walled Carbon Nanotube Dispersion

Taeheon Lee,[a] Jaehyun Park,[a] Kyungho Kim,[a] Aruna Kumar Mohanty,[a] Byoungjae Kim,[a] Jong Hun Han,[b] Heung Bae Jeon,[c] Young Sil Lee,[d,*] and Hyun-jong Paik[a,*]

We designed and synthesized a polymeric dispersant for use with single-walled carbon nanotubes (SWCNTs). *Poly*((furfuryl methacrylate)-*co*-(2-(dimethylamino)ethyl methacrylate)) (*p*(FMA-*co*-DMAEMA)) was synthesized, and its solubility tuned by the quaternization of a tertiary amine. Quaternized *p*(FMA-*co*-DMAEMA) (*p*(FMA-*co*-QDMAEMA)) changed the dispersibility of SWCNTs in various polar solvents, such as ethylene glycol (EG), methanol (MeOH), water and dimethylformamide (DMF). The chemical structures of the synthesized and modified polymeric dispersants were confirmed using ^{1}H NMR. The dispersion quality of SWCNTs by *p*(FMA-*co*-QDMAEMA) was estimated using a particle stability analyzer, zeta-potential, UV-vis-NIR spectroscopy, transmission electron microscopy, and atomic force microscopy. The diameters and degree of defects of dispersed SWCNTs were estimated using Raman spectroscopy. Dispersed SWCNTs in EG and MeOH display heights between 1.45 and 1.78 nm and a diameter of 1.17 nm, which corresponds to 1 or 2 bundled SWCNTs.

1. Introduction

Since their discovery, carbon nanotubes (CNTs)[1] have generated great interest because of their exceptional properties. In particular, single-walled carbon nanotubes (SWCNTs) are considered to be a promising material for various applications in electronics[2-7], sensors[8, 9], polymer reinforcements[10, 11], yarns[12, 13], and biomedical[14-16] applications. However, the inherent properties of CNTs are often hidden because CNTs in their primitive state exist as bundles, which is caused by strong π-π intertube interactions[17]. Therefore, the dispersion of bundled CNTs is a key technique to establish compatibility with various technologies. Overall, two broad categories of methods have been widely used for the separation and solubilization of CNTs: covalent and non-covalent dispersion[18, 19]. Non-covalent methods are realized via enthalpy and/or entropy driven interactions between a CNT and a dispersant [20]. In this manner, CNTs have been dispersed by a variety of species, including small molecular surfactants[21], polymeric dispersants[22-25] and DNA[26, 27]. Non-covalent dispersion methods using surfactants could minimize the introduction of defects compared with the covalent functionalization of CNTs[28]. However, the high energy input required to disperse CNTs with small molecular surfactants (e.g., sodium dodecyl sulfonate (SDS)) could shorten SWCNTs from their pristine length to under 1 μm[29, 30]. In contrast to small molecular surfactants, a polymeric dispersant, which contains both an absorbable group (anchoring group) and a solubility improving group (stabilizer), required less energy to exfoliate CNTs. This action resulted from an entropy penalty function and thus prevented the aggregation of CNTs more effectively under mild conditions[31-33]. Therefore, it is desirable to design polymeric surfactants for the dispersion of CNTs.

In our previous report[32], we prepared the polymer *poly*(furfuryl methacrylate-*co*-2-(dimethylamino)ethyl methacrylate) (*p*(FMA-*co*-DMAEMA)) for the dispersal of SWCNTs in tetrahydrofuran (THF). The dispersed SWCNTs exhibited a high aspect ratio with a length and diameter of 2.0 μm and 3.9 nm, respectively. However, THF was the only solvent that could disperse SWCNTs and *p*(FMA-*co*-DMAEMA) well, which indicated an inherent limitation. The preparation of stable SWCNTs dispersions with different solvents is essential to broaden the use of this material to applications such as coating substrates that have different types of surface properties.

In this study, the synthesized *p*(FMA-*co*-DMAEMA) was tuned by a simple conversion of the tertiary amine group of the polymer structure to a quaternary amine, increasing the polymer's affinity towards different solvents. Furthermore, the quaternized group generates a charge-charge repulsion between the dispersants absorbed on CNTs, which enhances the dispersion stability[34]. The quaternization of the amine in *p*(FMA-*co*-DMAEMA) was confirmed by ^{1}H NMR and

[a] Department of Polymer Science and Engineering, Pusan National University, San 30 Jangjeon2 dong, Geumjeong-gu, Busan 609-735, Korea
[b] School of Applied Chemical Engineering, Chongnam National University, 77 Yongbong-ro, Buk-gu, Gwangju 500-757, Korea
[c] Department of Chemistry, Kwangwoon University, 20, Gwangun-ro, Nowon-gu, Seoul 139-701, Korea
[d] ICT Convergence Research Center, Kumoh National Institute of Technology, 1 Yangho-dong, Gumi, Gyeongbuk 730-701, Korea

quantitatively calculated from the peak integral ratio. The quaternized *p*(FMA-*co*-DMAEMA), named *p*(FMA-*co*-QDMAEMA), efficiently dispersed SWCNTs in various polar solvents, such as ethylene glycol (EG), methanol(MeOH), water, and dimethylformamide (DMF). Dispersed SWCNTs solution with *p*(FMA-*co*-QDMAEMA) were investigated for their dispersion stability and dispersion state by particle stability analysis, UV-vis-NIR spectroscopy, transmission electron microscopy (TEM) and atomic force microscopy (AFM). Additionally, Raman spectroscopy was employed to find the diameters and degree of defects introduced in the dispersed SWCNTs during ultrasonication.

2. Experimental

2.1 Materials

SWCNTs (1.0–1.2 nm in diameter, 5–20 μm in length) made by an arc-discharge method were purchased from Nano Solution Co., Ltd. (Korea). Furfuryl methacrylate (FMA, 97%, Sigma-Aldrich) and 2-(dimethylamino)ethyl methacrylate (DMAEMA, 98%, TCI chemicals) were purified before use by passage through an alumina column to remove inhibitors. Copper(I) bromide (CuBr, 99%, Sigma-Aldrich) was purified by stirring with glacial acetic acid, followed by filtering and washing the resulting solid three times with methanol and two times with diethyl ether. The solid was then dried under vacuum for 2 days. Ethyl 2-bromoisobutyrate (EBiB, 99%, Sigma-Aldrich), 4,4′-dinonyl-2,2′-dipyridyl (dNbpy, 97%, Sigma-Aldrich), tetrahydrofuran (THF, 99.8%, J.T. Baker), ethylene glycol (EG, 99.5%, TCI chemicals), dimethylformamide (DMF, 99.5%, TCI chemicals) and methanol (MeOH, 99.8%, Sigma-Aldrich) were used as-received.

2.2 Instruments

The number average molecular weight (M_n) and molecular weight distribution (M_w/M_n) were determined using gel permeation chromatography (GPC) calibrated with poly(methyl methacrylate) (PMMA) standards. The chromatograph was equipped with an Agilent 1100 pump, a RID detector, and PSS SDV (5 μm; 10^5, 10^3, and 10^2 Å; 8.0 × 300.0 mm) columns. ^{1}H NMR spectra were obtained using a 500 MHz Agilent Superconducting FT-NMR spectrometer with chloroform-d as the solvent. The dispersion stability of the SWCNT solutions was determined using a Turbiscan LAB dispersion stability analyzer (Formulaction). The electrophoretic mobility of the SWCNTs samples was measured as a function of pH at 25 °C using a Zetasizer (Malvern Nanosizer ZS, Malvern Instruments, UK) in a standard capillary electrophoresis cell (DTS1070). The transmittance profiles obtained from the dispersion stability analyzer were assessed as a function of time (scans every 2 hours for 2 days) and of sample height (5–30 mm). The UV-vis-NIR spectra of the SWCNT solutions after centrifugation were measured using Cary 5E (Varian) spectrophotometer with 1 nm steps. The de-bundled SWCNTs in the dispersion solution were characterized using transmission electron microscopy (with an H-7600 TEM from Hitachi) and atomic force microscopy (AFM). Droplets of the solution were applied directly to carbon-coated copper grids. Non-contact (tapping) AFM was performed with an n-tracer SPM (Nanofocus). The cantilever was made of silicon with a resonant frequency of approximately 320 kHz and a nominal radius of curvature of l 8 nm. Images were obtained at room temperature and in air. The structural characteristics of the SWCNT sheets were investigated using an NTEGRA Spectra confocal Raman spectrometer (NT-MDT), with an excitation wavelength of 532 nm.

2.3 Synthesis of *p*(FMA-*co*-DMAEMA)

p(FMA-*co*-DMAEMA) was synthesized using atom transfer radical polymerization (ATRP) from DMAEMA and FMA with the CuBr/dNbpy catalyst and EBiB as an initiator. DMAEMA (5.47 mL, 32.4 mmol), FMA (10.0 mL, 64.8 mmol), EBiB (160 μL, 1.08 mmol) and anisole (8.00 mL) were deoxygenated through bubbling with N_2 for at least 30 min. dNbpy (338 mg, 2.16 mmol) and CuBr (124 mg, 0.87 mmol) were quickly added to the 50-mL Schlenk flask. The flask was sealed with a glass stopper, and the cycle of vacuum and filling with nitrogen was repeated three times. After this process, regardless of the order, the degassed liquid materials (except for the initiator) were charged into the Schlenk flask; finally, the initiator was added to the mixture. The mixture was stirred for 100 min at 50°C under an N_2 atmosphere and then diluted with THF and passed through a neutral alumina column to remove the copper catalyst. After the column separation, *p*(FMA-*co*-DMAEMA) was isolated in hexane and dried under vacuum at room temperature for 24 h. (M_n = 14,800 and M_w/M_n = 1.42 were determined using GPC)

2.4 Quaternary ammonium modification of *p*(FMA-*co*-DMAEMA)

The quaternized polymer *p*(FMA-co-QDMAEMA) was synthesized from synthesized *p*(FMA-*co*-DMAEMA). The typical procedure is as follows: 0.5 g of *p*(FMA-*co*-DMAEMA) (containing 1.02 mmol of DMAEMA) was dissolved in DMF (1 mL) in a round bottom flask under stirring at room temperature. Iodo methane (63.6 μL; 1.02 mmol) was added to the solution and allowed the reaction to continue for 24 h. The quaternized polymer was twice precipitated in isopropyl ether and dried under vacuum for 48 h.

2.5 Dispersions of SWCNTs using the polymeric dispersant

The polymeric dispersants (40.0 mg) were dissolved in 40.0 mL of solvent (EG, MeOH, THF, water, or DMF). The SWCNTs (4.0 mg) were added to this polymer solution and dispersed by sonication in a bath-type sonicator (WUC-D22H, DAIHAN Scientific Co. 40 kHz, 400 Watt) for 3 h. The dispersed SWCNT solution was centrifuged at 10,000 rpm for 15 min to remove both bundled SWCNTs and the metal catalyst[35]. The well-dispersed SWCNT solution was obtained as the supernatant.

3. Results and discussion

3.1 Design and characterization of the polymeric dispersants

With respect to the synthesized polymeric dispersant, the design of chemical structure is important for determining the material properties. *P*(FMA-*co*-DMAEMA) has limited solubility in polar solvents. To enhance the solubility of *p*(FMA-*co*-DMAEMA), simple chemistry was applied through the conversion of a tertiary amine to a quaternary with charge. The synthesis and modification of the polymeric dispersant are shown in Scheme 1. After quaternization, the dispersant's solubility characteristics towards a range solvents changed due to the positive charge center in the polymer structure, as summarized in Table 1. The structure of synthesized *p*(FMA-*co*-DMAEMA) was confirmed by ^{1}H NMR, as shown in Figure 1(a). The composition of the individual monomer moieties in the polymer structure was calculated by comparing the integration ratio of the furan proton peak at δ = 7.4 ppm in FMA to the methylene (-CO_2CH_2-) proton peak (at δ = 4.02 ppm) in DMAEMA. Quaternization of the amine in the DMAEMA unit was clearly confirmed by the peak shift in ^{1}H NMR for *p*(FMA-*co*-QDMAEMA) in Figure 1(b). After amine quaternization, the methylene (-CO_2CH_2-) proton peak of the DMAEMA moiety, which appeared at δ = 4.02 ppm for *p*(FMA-*co*-DMAEMA), shifts to δ = 4.34 ppm in *p*(FMA-*co*-QDMAEMA). The degree of quaternization calculated from the ^{1}H NMR peak integration was 94%.

Scheme 1.

Figure 1.

Table 1.

3.2 Characterization of the SWCNT dispersion

Before quaternization, *p*(FMA-*co*-DMAEMA) with SWCNTs readily dispersed only in THF, that is, we observed rapid sedimentation of SWCNTs immediately after sonication for all other polar solvents. With EG, we observed the partially dispersed SWCNTs by visual inspection, but a considerable number of bundles as expected in the sample. However, after quaternization and sonication, *p*(FMA-*co*-QDMAEMA) showed good dispersibility of SWCNTs, as evidenced by the presence of a homogeneous dark solution in various polar solvents, as shown in Figure 2. The dispersion stability of SWCNTs was investigated using a particle stability analyzer over a 2 day period. As shown in Figure 3, the transmittance of well-dispersed SWCNT solutions hardly changed after 2 days with the highest observed change in DMF. After 2 days, the changes in transmittance were (in ascending order) 0.085 (in MeOH), 0.149 in EG), 1.29 (in water), 1.39 (in THF with non-quaternized dispersant)[32] and 1.78 (in DMF), indicating the polar solvent versatility of the newly synthesized polymeric dispersant .

Figure 2.

Figure 3.

Furthermore, to estimate the charge-charge repulsion effect of dispersion, the zeta (ζ)-potential was measured for p(FMA-co-QDMAEMA), SWCNT, and p(FMA-co-QDMAEMA) dispersed SWCNT in various solutions, respectively. The p(FMA-co-QDMAEMA) absorbed on SWCNT surface has positive charge which leads to electrostatic repulsion between the exfoliated SWCNTs. The electrical potential at the SWCNT surface can be measured by ζ–potential. The results of the ζ-potential in table 2 indicated the effective SWCNT dispersibility and stability. After mixing of SWCNT and polymeric dispersant, ζ-potential were increase than only SWCNT or dispersant because absorbed polymer makes dispersed SWCNTs high surface charge. Therefore this results indicate much polymer absorbed on SWCNT surface and mobile not only each component but p(FMA-co-QDMAEMA) wrapping SWCNTs. Therefore the values of surface charge are higher than each polymer or SWCNT in solutions. Also the order of the ζ-potential value of p(FMA-co-QDMAEMA) dispersed SWCNTs is in the order of MeOH (47.3 mV) > EG (43.5 mV) > water (40.9 mV) > DMF (36.2 mV) which is almost consistent with the order of the dispersion stability as shown in Figure 3.

Table 2

TEM was used to study the dispersion states of SWCNTs in different solvents (Figure 4). After centrifugation, SWCNTs dispersed in water or DMF solutions were observed as nanotube bundles. In MeOH, the dispersion contained long SWCNTs that were only a few nanotubes per isolated bundle. However, the EG solution provided the best results with well-dispersed SWCNTs of long length and very thin thicknesses, as shown in Figure 4(a). This result is in comparison to the dispersion quality of SWCNTs in the EG using *p*(FMA-*co*-DMAEMA) before quaternization, as mentioned above. The main chain of *p*(FMA-*co*-DMAEMA) remained important for preparing good SWCNT dispersions, even though it was modified. Additionally, AFM was used to determine the presence of individual SWCNTs or of small bundles. AFM maps and height profiles of SWCNTs are shown in Figure 5. The height profiles of dispersed SWCNTs, which indicate the degree of exfoliation, are shown in figure 5(b), (d), (f), and (h). Based on these data, the average values of height were determined to be 1.45 (±0.59) nm in EG, 1.78 (±0.69) nm in MeOH, 8.5 (±4.3) nm in water and 12.9 (±5.7) nm in DMF. These results showed good dispersion of SWCNTs as few-nanotube bundles, which correlated well with the TEM results. In particular, SWCNTs iin EG and MeOH showed better dispersion than our previous result, of 2.92 (±1.78, in THF with the non-modified polymer) nm[32]. Furthermore, SWCNTs in EG and MeOH appeared to almost exfoliate individually, while larger SWCNT aggregates were observed in water and DMF.

Figure 4.

Figure 5.

To investigate the dispersion quality of SWCNTs in different solvents, well dispersed SWCNT solutions were measured by UV-vis-NIR spectrophotometry. UV-vis-NIR absorption spectroscopy is a powerful tool for the characterization of SWCNT dispersion efficiency[36]. In the UV-Vis region, individual SWCNTs show characteristic absorption bands corresponding to van Hove singularities. In contrast, the tunneling of carriers between bundled CNTs reduces the intensity of these absorption bands due to the quenching of the photoluminescence properties[17, 18]. Figure 6 shows the UV-vis-NIR absorptions of the dispersed SWCNT solutions in the 400-1300 nm region. The peaks at 900-1300 nm were assigned to the first van Hove transitions of semiconducting SWCNTs (S11), the peaks found between 550-800 nm were due to the second van Hove transitions of semiconducting SWCNT (S22), and the features between 400-550 nm were attributed to the first van Hove transitions of metallic SWCNT (M11)[37]. The relatively well-resolved absorbance spectra of SWCNT with *p*(FMA-*co*-QDMAEMA) in EG and MeOH represent sharp interband transitions, revealing the superior dispersion of individual SWCNTs. Decreases in the intensities of these absorption bands indicated a reduced dispersibility of solvents in the following order: EG, MeOH, water and DMF. Thus, the solvent order of SWCNT and *p*(FMA-*co*-QDMAEMA) dispersions, as determined by UV-vis-NIR spectroscopy, correlated well with the results of TEM and AFM.

Figure 6.

The introduction of defects to SWCNTs due to the use of high-power ultrasonication with non-covalent methods of dispersion have remained a concern, even though non-covalent dispersions yield less defects in SWCNT structures than covalent functionalization. High-powered ultrasonication can shorten the length of SWCNTs from a few micrometers to a few hundred nanometers. In this context, Raman spectroscopy has been successfully used to characterize the properties of and determine the level of defects in SWCNTs. Figure 7 shows the Raman spectra for dispersions in different solvents that display the characteristic peaks of SWCNTs. The peak at 188 cm^{-1} was ascribed to the radial breathing mode (RBM) caused by the expansion and the contraction of the nanotube. The peak at 1287 cm^{-1} represents the disorder-induced mode D. While, the peaks near 1583 cm^{-1} are assigned to the G band, arising from vibrations along the axis and around the circumference of the tube, and the G' band, which is an overtone of the D peak. The RBM frequency (ω_{RBM}) is especially important for the determination of the diameter distribution of SWCNTs[38,39] and the structural assignments of optical transitions in SWCNTs[40-42]. The RBM frequency can be empirically related to the diameter of the SWCNT by

$\omega_{RBM} = \frac{C_1}{d}$, equation (1)

where d is the diameter of the carbon nanotube and C_1[37] is equal to 223.75. The two main peaks of the RBM were observed for dispersed SWCNTs at approximately 164.40 and 188.81 cm^{-1}. From these results, the diameters of SWCNTs, as calculated by equation (1), were in the range of 1.36 to 1.17 nm, which is slightly larger than the size provided by the manufacturer. A shift in RBM frequencies to higher wavenumbers is a known effect of the high pressure applied to SWCNTs[43-45]. The coating of SWCNTs with a polar solvent that is capable of hydrogen bonding should give rise to a quasi-high pressure effect on the RBM band. In our case, the RBM frequencies for SWCNTs dispersed in all solvents with the polymeric surfactant shift to lower wavenumbers. The adsorbed polymeric surfactant repels solvent molecules from the SWCNT surface. Because the D band is related to defects in the nanotube structures, as well as the amorphous carbon content[46], the Raman D:G peak ratio was also measured, as it related to the purity of SWCNTs in the solutions. The D/G ratio was determined to be in the range of 0.017 to 0.036 for the tested solvents. This result indicates the successful dispersion of SWCNTs without strongly damaging their structures. Although the defect levels of SWCNTs in all of the solvents used in this study are relatively low, the D/G value of SWCNTs with polymeric surfactant in EG are higher than that in other solvents, which indicates an increased amount of defective SWCNTs. When comparing the TEM images of dispersed SWCNTs in Figure 4, the length of SWCNTs from EG are relatively shorter than that observed for other solvents.

Figure 7.

Table 2.

4. Conclusions

Bundled SWCNTs cannot display their intrinsic properties, although SWCNTs have been considered to be a promising material for various applications. To utilize their superb properties, proper dispersion of SWCNTs is crucial key to overcome the strong intertube interactions. Previously synthesized *p*(FMA-*co*-DMAEMA) could disperse SWCNT only in THF, which limited its application. Therefore, the dispersant was modified, using simple organic chemistry, by the quaternization of the amine group in the polymer. After quaternization, the polymer not only has a charge but also displays solubility in various polar solutions. Using the tuned polymeric dispersant *p*(FMA-*co*-QDMAEMA), SWCNTs could be uniformly solubilized in various solvents, such as EG, MeOH, water, and DMF; the dispersion quality was characterized by a number of techniques. According to these results, *p*(FMA-*co*-QDMAEMA) had a remarkable dispersibility of SWCNTs in the tested solvents. In particular, EG dispersed SWCNTs have an average height and diameter of 1.45 (±0.59) nm and 1.17 nm, respectively, which indicate that the number of bundled SWCNTs is essentially 1 or 2. Individually dispersed SWCNTs can be used in the field of the electronics as a low-threshold concentration material.

Acknowledgements

This work was supported by Basic Science Research Program through the National Research Foundation of Korea (NRF) grant funded by the Korean government (MSIP) (2013R1A2A2A01068818), the Industrial Strategic Technology Development Program (10045051) funded by the Ministry of Trade, Industry and Energy (MOTIE) of Korea and BK21 PLUS Centre for Advanced Chemical Technology (21A20131800002).

References

1. S. Iijima, *Nature*, 1991, **354**, 56-58.
2. T. Kurkina, A. Vlandas, A. Ahmad, K. Kern and K. Balasubramanian, *Angew. Chem. Int. Ed.*, 2011, **50**, 3710-3714.
3. S. Park, M. Vosguerichian and Z. Bao, *Nanoscale*, 2013, **5**, 1727-1752.
4. C. Biswas and Y. H. Lee, *Adv. Funct. Mater.*, 2011, **21**, 3806-3826.
5. W. J. Yu, S. Y. Lee, S. H. Chae, D. Perello, G. H. Han, M. Yun and Y. H. Lee, *Nano Lett.*, 2011, **11**, 1344-1350.
6. J. T. Han, J. S. Kim, H. D. Jeong, H. J. Jeong, S. Y. Jeong and G.-W. Lee, *J. Mater. Chem.*, 2010, **20**, 8557-8562.
7. J. W. Jo, J. W. Jung, J. U. Lee and W. H. Jo, *ACS Nano*, 2010, **4**, 5382-5388.
8. B. L. Allen, P. D. Kichambare and A. Star, *Adv. Mater.*, 2007, **19**, 1439-1451.
9. C. Robert, J. F. Feller and M. Castro, *ACS Appl. Mater. Interfaces*, 2012, **4**, 3508-3516.
10. M. M. J. Treacy, T. W. Ebbesen and J. M. Gibson, *Nature*, 1996, **381**, 678-680.
11. M. Moniruzzaman and K. I. Winey, *Macromolecules*, 2006, **39**, 5194-5205.
12. K. Koziol, J. Vilatela, A. Moisala, M. Motta, P. Cunniff, M. Sennett and A. Windle, *Science*, 2007, **318**, 1892-1895.
13. W. Lu, M. Zu, J.-H. Byun, B.-S. Kim and T.-W. Chou, *Adv. Mater.*, 2012, **24**, 1805-1833.
14. C. Cha, S. R. Shin, N. Annabi, M. R. Dokmeci and A. Khademhosseini, *ACS Nano*, 2013, **7**, 2891-2897.
15. C. Hu and S. Hu, *J. Sens.*, 2009, 1-40.
16. E. Heister, E. W. Brunner, G. R. Dieckmann, I. Jurewicz and A. B. Dalton, *ACS Appl. Mater. Interfaces*, 2013, **5**, 1870-1891.
17. V. M. F. L. De, S. H. Tawfick, R. H. Baughman and A. J. Hart, *Science*, 2013, **339**, 535-539.
18. P.-C. Ma, N. A. Siddiqui, G. Marom and J.-K. Kim, *Composites Part A*, 2010, **41**, 1345-1367.
19. S. W. Kim, T. Kim, Y. S. Kim, H. S. Choi, H. J. Lim, S. J. Yang and C. R. Park, *Carbon*, 2012, **50**, 3-33.
20. F. Tsuyohiko and N. Naotoshi, *Science and Technology of Advanced Materials*, 2015, **16**, 024802.
21. K. Yang, Z. Yi, Q. Jing, R. Yue, W. Jiang and D. Lin, *Chin. Sci. Bull.*, 2013, **58**, 2082-2090.
22. P. Bilalis, D. Katsigiannopoulos, A. Avgeropoulos and G. Sakellariou, *RSC Advances*, 2014, **4**, 2911-2934.
23. B.-S. Kim, D. Kim, K.-W. Kim, T. Lee, S. Kim, K. Shin, S. Chun, J. H. Han, Y. S. Lee and H.-j. Paik, *Carbon*, 2014, **72**, 57-65.
24. K. Y. Cho, Y. S. Yeom, H. Y. Seo, Y. H. Park, H. N. Jang, K.-Y. Baek and H. G. Yoon, *ACS Appl. Mater. Interfaces*, 2015, **7**, 9841-9850.
25. K. K. Kim, S. M. Yoon, J. Y. Choi, J. Lee, B. K. Kim, J. M. Kim, J. H. Lee, U. Paik, M. H. Park, C. W. Yang, K. H. An, Y. Chung and Y. H. Lee, *Adv. Funct. Mater.*, 2007, **17**, 1775-1783.
26. M. Zheng, A. Jagota, E. D. Semke, B. A. Diner, R. S. McLean, S. R. Lustig, R. E. Richardson and N. G. Tassi, *Nat Mater*, 2003, **2**, 338-342.
27. C. Hu, Y. Zhang, G. Bao, Y. Zhang, M. Liu and Z. L. Wang, *J. Phys. Chem. B*, 2005, **109**, 20072-20076.
28. T. J. Simmons, J. Bult, D. P. Hashim, R. J. Linhardt and P. M. Ajayan, *ACS Nano*, 2009, **3**, 865-870.
29. P. Vichchulada, M. A. Cauble, E. A. Abdi, E. I. Obi, Q. Zhang and M. D. Lay, *J. Phys. Chem. C*, 2010, **114**, 12490-12495.
30. A. Lucas, C. Zakri, M. Maugey, M. Pasquali, P. v. d. Schoot and P. Poulin, *J. Phys. Chem. C*, 2009, **113**, 20599-20605.
31. C. Y. Hu, Y. J. Xu, S. W. Duo, R. F. Zhang and M. S. Li, *J. Chin. Chem. Soc.*, 2009, **56**, 234-239.
32. T. Lee, B. Kim, S. Kim, J. H. Han, H. B. Jeon, Y. S. Lee and H.-j. Paik, *Nanoscale*, 2015, **7**, 6745-6753.
33. S. Luo, T. Liu, S. M. Benjamin and J. S. Brooks, *Langmuir*, 2013, **29**, 8694-8702.
34. Z. Sun, V. Nicolosi, D. Rickard, S. D. Bergin, D. Aherne and J. N. Coleman, *J. Phys. Chem. C*, 2008, **112**, 10692-10699.
35. A. Yu, E. Bekyarova, M. E. Itkis, D. Fakhrutdinov, R. Webster and R. C. Haddon, *J. Am. Chem. Soc.*, 2006, **128**, 9902-9908.
36. P. Kim, T. W. Odom, J.-L. Huang and C. M. Lieber, *Phys. Rev. Lett.*, 1999, **82**, 1225-1228.
37. T. Liu, G. Xu, J. Zhang, H. Zhang and J. Pang, *Colloid. Polym. Sci.*, 2013, **291**, 691-698.
38. L. Alvarez, A. Righi, T. Guillard, S. Rols, E. Anglaret, D. Laplaze and J.-L. Sauvajol, *Chem. Phys. Lett.*, 2000, **316**, 186-190.
39. H. Kuzmany, W. Plank, M. Hulman, C. Kramberger, A. Grüneis, T. Pichler, H. Peterlik, H. Kataura and Y. Achiba, *Eur. Phys. J. B*, 2001, **22**, 307-320.
40. S. M. Bachilo, M. S. Strano, C. Kittrell, R. H. Hauge, R. E. Smalley and R. B. Weisman, *Science*, 2002, **298**, 2361-2366.
41. P. T. Araujo, S. K. Doorn, S. Kilina, S. Tretiak, E. Einarsson, S. Maruyama, H. Chacham, M. A. Pimenta and A. Jorio, *Phys. Rev. Lett.*, 2007, **98**, 067401.
42. P. T. Araujo, A. Jorio, M. S. Dresselhaus, K. Sato and R. Saito, *Phys. Rev. Lett.*, 2009, **103**, 146802.
43. U. D. Venkateswaran, D. L. Masica, G. U. Sumanasekera, C. A. Furtado, U. J. Kim and P. C. Eklund, *Physical Review B*, 2003, **68**, 241406.
44. S. Utsumi, M. Kanamaru, H. Honda, H. Kanoh, H. Tanaka, T. Ohkubo, H. Sakai, M. Abe and K. Kaneko, *J. Colloid Interface Sci.*, 2007, **308**, 276-284.
45. U. D. Venkateswaran, A. M. Rao, E. Richter, M. Menon, A. Rinzler, R. E. Smalley and P. C. Eklund, *Physical Review B*, 1999, **59**, 10928-10934.
46. M. S. Dresselhaus, G. Dresselhaus, R. Saito and A. Jorio, *Physics Reports*, 2005, **409**, 47-99.

List of schemes

Scheme 1. Synthesis and modification of the polymeric dispersants

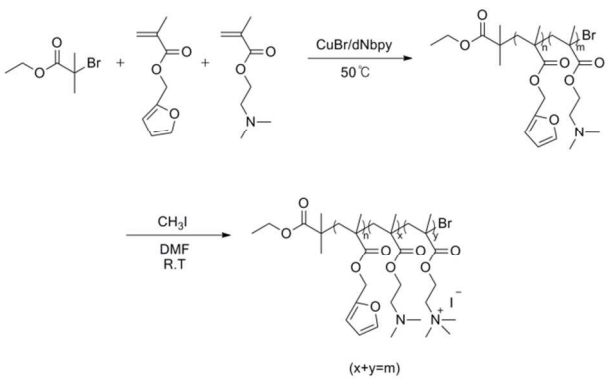

Scheme 1. Synthesis and modification of the polymeric dispersants

List of tables

Table 1. Solubility characteristics of the polymeric dispersants before and after modification

Polymeric dispersant	EG	MeOH	THF	water	DMF
***p*(FMA-*co*-DMAEMA)**	insoluble(-)	insoluble(-)	soluble(+)	insoluble(-)	soluble(-)
***p*(FMA-*co*-QDMAEMA)**	soluble(+)	soluble(+)	insoluble(-)	partially soluble(+)	soluble(+)

(+) indicates dispersion of SWCNTs; and (-) indicates aggregation of SWCNTs

Table 2. Data of ζ -potential values for various solvents

	EG (mV)	MeOH (mV)	Water (mV)	DMF (mV)
P(FMA-co-QDMAEMA)	15.5	18.8	34.2	15.6
SWCNT	-5.28	8.79	-9.09	-19.4
P(FMA-co-QDMAEMA)/SWCNT	43.5	47.3	40.9	36.2

Table 3. Information of dispersion quality, diameters and degree of defects for the dispersed SWCNTs

Solvent	ΔT (%)[a)]	Average Height (nm)[b)]	RBM (cm^{-1})	Diameter (nm)[c)]	I_D/I_G
EG	0.149	1.45 (±0.59)	190.69 (166.28)	1.17 (1.35)	0.036
MeOH	0.085	1.78 (±0.69)	188.81 (164.40)	1.19 (1.36)	0.019
Water	1.29	8.5 (±4.3)	188.81 (164.40)	1.19 (1.36)	0.017
DMF	1.78	12.9 (±5.7)	188.81 (164.40)	1.19 (1.36)	0.019

a) Estimated by a particle stability analyzer
b) Observed by the height profile from an AFM image
c) Calculated using equation (1)

List of figures

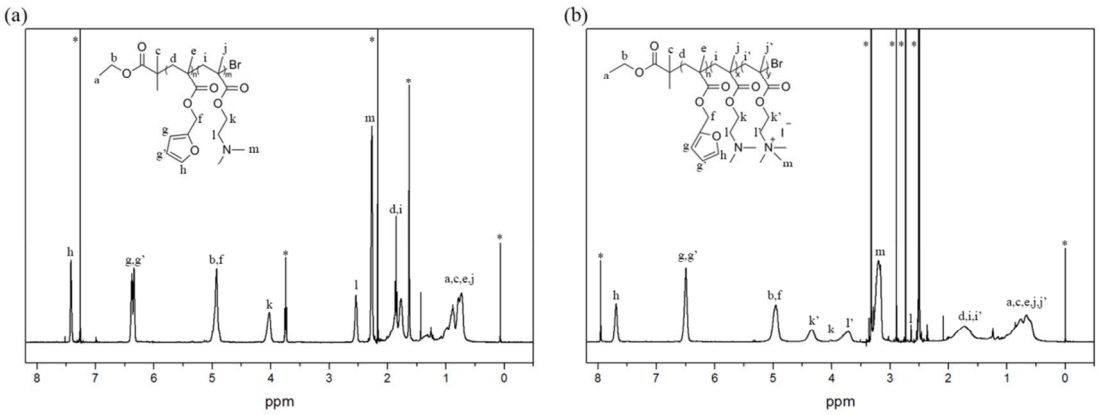

Figure 1. ^{1}H NMR spectra of (a) *p*(FMA-*co*-DMAEMA) and (b) *p*(FMA-*co*-QDMAEMA).

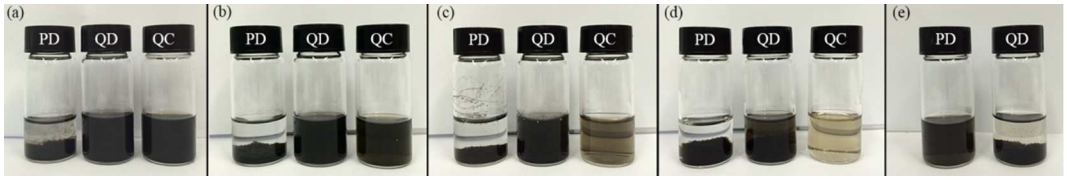

Figure 2. Photographs of various SWCNT solutions. PD used for the polymeric dispersant before quaternization, QD used for quaternized dispersants and QC indicated the supernatant of the QD solution after centrifugation; (a) EG, (b) MeOH, (c) water, (d) DMF and (e) THF.

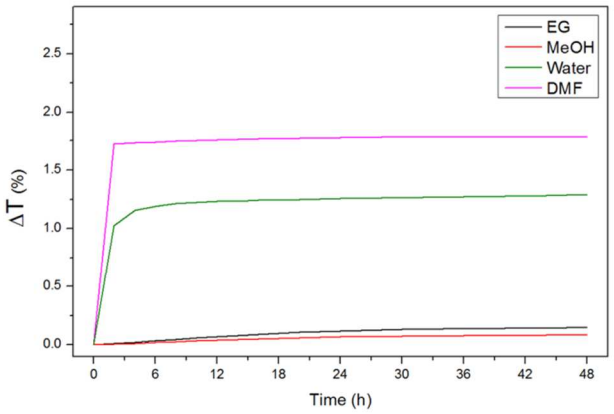

Figure 3. Transmittance changes in the SWCNT dispersions for 2 days.

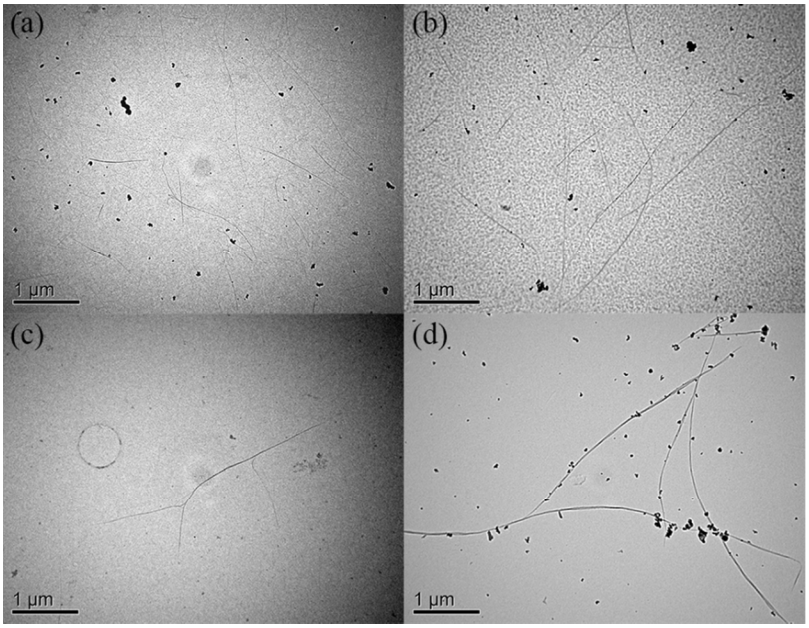

Figure 4. TEM images of dispersed SWCNTs in various solvents: (a) EG, (b) MeOH, (c) water, and (d) DMF.

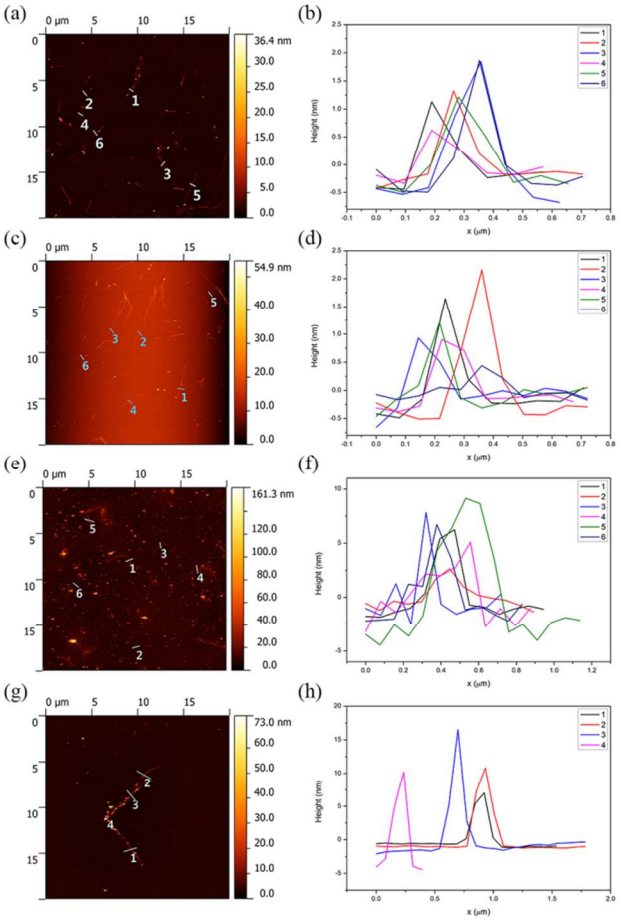

Figure 5. AFM images and height profiles of dispersed SWCNTs in (a-b) EG, (c-d) MeOH, (e-f) water, and (g-h) DMF.

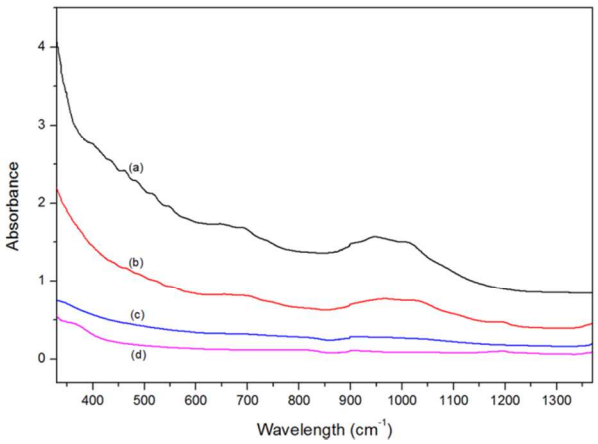

Figure 6. UV-vis-NIR absorptions for dispersions of SWCNTs with the polymeric surfactant *p*(FMA-*co*-QDMAEMA) in different solvents (a) EG, (b) MeOH, (c) water, (d) and DMF.

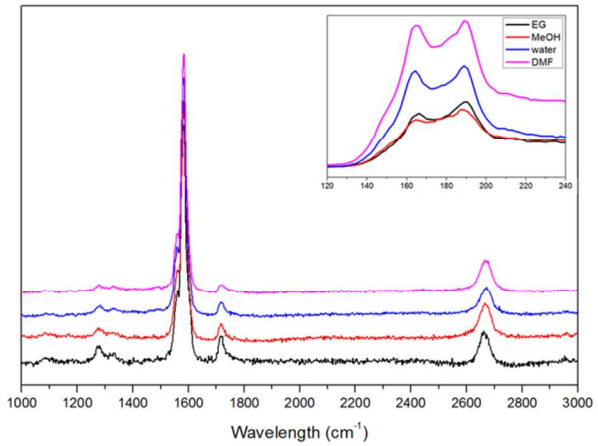

Figure 7. Raman spectra of dispersed SWCNTs in various solvents. The inserted legend indicates the RBM region.